American Mineralogist, Volume 69, pages 277–282, 1984

On spinodal decomposition in Fe-free pyroxenes

CAROL M. JANTZEN

E. I. du Pont de Nemours & Co.
Savannah River Laboratory
Aiken, South Carolina 29808

Abstract

Theoretical treatments of spinodal decomposition are kinetic models of the decomposition mechanism. Use of morphologic or textural arguments to determine mechanistic changes during the solidification of alloy, ceramic, or mineralogic systems can be misleading. The literature on spinodal mechanisms in Fe-free pyroxene systems forms a consistent picture when the experimental data for iron-free and iron-enriched pyroxenes are compared and related to the more recent mathematical treatments of late stage spinodal decomposition. Recognition of spinodal coarsening via a $t^{1/3}$ rate law and coarsening of coherent nucleation at $t^{1/3}$ may elucidate positioning of the coherent spinodal and the coherent solvus in the iron-free pyroxene system.

Decompositon morphologies

Morphologic considerations have often been employed to delineate spinodal decomposition. A specific repetitive spacing or mutual connectivity between the conjugate product phases has been cited as evidence for the operation of the spinodal process. Clearly, the repetitive spacing of exsolution lamellae fall into this category and spinodal decomposition has been invoked as one possible mechanism for exsolution in pyroxenes (McCallister and Yund, 1975).

Phase connectivity and periodicity cannot be considered to be unequivocal evidence of spinodal decomposition (Ardell et al., 1966; Seward et al., 1968; Herman and MacCrone, 1971; McCallister and Yund, 1977; Jantzen and Herman, 1978). Anisotropic strain fields can give rise to periodicity (Ardell et al., 1966), discontinuous cellular structures can give rise to lamellar structures (Fine, 1964; Herman and MacCrone, 1971; Tarshis et al., 1973), while eutectic solidification (Kraft, 1973; Shewmon, 1969), eutectoid decomposition (Mangonon et al., 1973; Mack, 1973) and discontinuous precipitation (Newkirk, 1973) can all give rise to lamellar structures.

Systems in which the volume fraction of each of the conjugate phases are comparable can also exhibit connectivity based on geometric arguments (Herman and MacCrone, 1971). Indeed, work on two systems in which the origin of modulated structures were investigated has demonstrated conclusively that spinodal composition was not the operational mechanism (Ardell et al., 1966; Seward et al., 1968).

Exsolution morphologies observed in both synthetic iron-rich and lunar pyroxenes have recently been ascribed to a variety of mechanisms which include two homogeneous exsolution mechanisms and heterogeneous nucleation, e.g., large heterogeneously distributed lamellae nucleate on dislocations or subgrain boundaries (Grove, 1982). Tweed structures in rapidly cooled pyroxenes have been attributed to decompositon by a spinodal mechanism while slower cooling rates (<10°C/hr) produce coarsening and cooling rates of 0.5°C/hr and 0.2°C/hr form large lamellae by homogeneous nucleation (Grove, 1982). Moreover, on slow cooling, heterogeneously nucleated lamellae on the equilibrium solvus may grow at elevated temperatures and subsequently decompose by a spinodal or nucleation and growth mechanism. Complex microscopic textures can, thereby, be produced over small temperature intervals (Grove, 1982).

The textural variations of the pyroxenes, as observed by McCallister and Yund (1975, 1977), should not be quoted as unequivocal evidence for an operative spinodal mechanism in Fe-free pyroxenes, as in, e.g., a recent review of pyroxene crystal chemistry by Cameron and Papike (1981). Morphologic studies are ambiguous unless kinetic studies of the evolution of the concentration profiles of the emerging phases with time are examined by the "microstructural sequence method" (Laughlin and Cahn, 1975) or by small-angle scattering techniques (Rundman and Hilliard, 1967).

Spinodal decomposition vis-a-vis nucleation and growth

The spinodal theories developed by Cahn (1962) and co-workers (Huston et al., 1966) are kinetic models. The use of morphologic arguments alone is, therefore, mis-

0003–004X/84/0304–0277$02.00

leading. Cameron and Papike (1981) address the issue of the similarity of spinodally coarsened structures to those of nucleation and growth; however, they merely quote the textural evidence of McCallister and Yund (1975) as evidence for a spinodal mechanism being operational in systems along the diopside–enstatite (Di–En) join.

Historically, Cameron and Papike's (1981) interpretations are based upon the earlier works of Yund and McCallister. Yund and McCallister (1970) first suggested that the textures of both exsolved pyroxenes and amphiboles were similar to perlite (eutectoid) structures in alloy systems and hence possibly formed by discontinuous precipitation. Cellular precipitation has also been proposed to explain rare exsolution microstructures in pyroxenes (Buseck et al., 1980). Subsequent experimentation by McCallister (1974a) on supersaturated solid solutions of Di annealed in the Pr_{ss} + Di_{ss} phase field from 10 to 300 hours suggested that the operative decomposition mechanism might be nucleation and growth by a continuous mode. Likewise, Champness and Lorimer (1973) found evidence supporting coherent nucleation and growth along the pseudobinary bronzite–augite solvus.

Examination of a ~54 mole% Di pyroxene with wide-angle X-ray diffraction (McCallister, 1974b), suggested that above 1300°C the decomposition appeared to be via a nucleation and growth mechanism, while at 1275°C decomposition appeared to proceed via a spinodal mode. McCallister and Yund (1975, 1977) used the morphologic irregular coherent lamellae observed in TEM at ~54 mole% Di (20 hours heat treatment at 1250°C) to suggest decomposition by a spinodal mechanism. The regular widely spaced lamellae observed in ~68 mole% Di compositions (1125°C for 697 hours) were attributed to decomposition by coherent nucleation and growth (Fig. 1).

Using the following data:

(1) the coherent spinodal of McCallister and Yund (1975, 1977) plotted on the entire phase diagram[1] for $CaMgSi_2O_6$(Di)–$Mg_2Si_2O_6$(En) in mole%;

(2) the estimated equilibrium consolute point of Yang (1973) at ~1450°C;

(3) the ΔT of ~110°C, calculated for this system by Fletcher and McCallister (1974);

(4) the exsolved (001) coherent solvus compositions and range of pyroxene compositions from kimberlites at an apparent quench temperature of 1000°C (McCallister and Nord, 1981); and

(5) a solvus calculated in this study from the experimentally determined spinodal curve by the technique of Cook and Hilliard (1965),

a coherent phase diagram can be plotted that is consistent with the available experimental data given above and in Figure 1. The dark circles represent the irregular type coherent lamellae of McCallister and Yund (1975, 1977), while the open circles and squares represent rare appearances of lamellae and/or lamellae whose spacings appear to be related to the supersaturation. The former could well represent coherent lamellae formed by spinodal decomposition while the latter represent coherent lamellae formed by nucleation and growth. Since the microstructural sequence method was not applied in these experiments, the unequivocal interpretation of the decomposition mechanism is not established.

Decomposition by a spinodal mode may well occur in iron-free pyroxenes along the Di–En join as demonstrated by the microstructural sequence method for iron-rich pyroxenes (Nord and McCallister, 1979; Buseck et al., 1980), but the experimental data of McCallister and Yund (1975, 1977) and McCallister (1978) is inconclusive.

Although small changes in composition can lead to a change in the type of phase separation, the proposed coherent spinodals of two iron-rich pseudobinary joins across the pyroxene quadrilateral at En/Fs = 2.0 (Lally et al., 1975) and En/Fs = 1.5 (Grove, 1982) have been projected onto the En–Di join for comparison (Fig. 1). Therefore, three pseudobinary miscibility gaps have been delineated in the pyroxene quadrilateral. Traversing across the quadrilateral toward the iron-free Eu–Di pyroxene join the critical temperature (T_c) shifts to lower temperature, the critical composition shifts to more Di-rich compositions, and the width of the proposed coherent spinodals appears to constrict. Although three pseudobinary coherent spinodals are suggested in the pyroxene quadrilateral and spinodal decomposition has been verified in iron-rich pyroxene systems, the decomposition of the pyroxenes along the Di–En join cannot be ascribed to a spinodal mechanism without further experimental verification.

Coarsening vs. late-stage spinodal decomposition

The kinetic treatments of coarsening in iron-free pyroxenes (McCallister, 1978; Buseck et al., 1980) and iron-enriched pyroxenes (Nord and McCallister, 1979; Nord, 1980) combined with the kinetic cooling rate data for iron-rich pyroxenes (Nord and McCallister, 1979; Grove, 1982) gives a thorough analysis of the genetic and geothermal history of pyroxene microstructures but does not address the relation of later-stage spinodal processes and coarsening.

The kinetics of the (001) exsolution in synthetic $Di_{54}En_{46}$ (McCallister, 1978) follow a $t^{1/3}$ coarsening law which Nord and McCallister (1979) and Nord (1980) attribute to the phenomena of "increasing decomposition wavelength with time at constant amplitude", e.g., the coherent solvus. Within the spinodal, early decomposition wavelengths must be constant with increasing time while composition differences increase with time (Laughlin and Cahn, 1975; Nord and McCallister, 1979): the

[1] McCallister and Yund (1975, 1977) only plotted one portion of the Di–En phase diagram making interpretation of the coherent and equilibrium phase relations difficult.

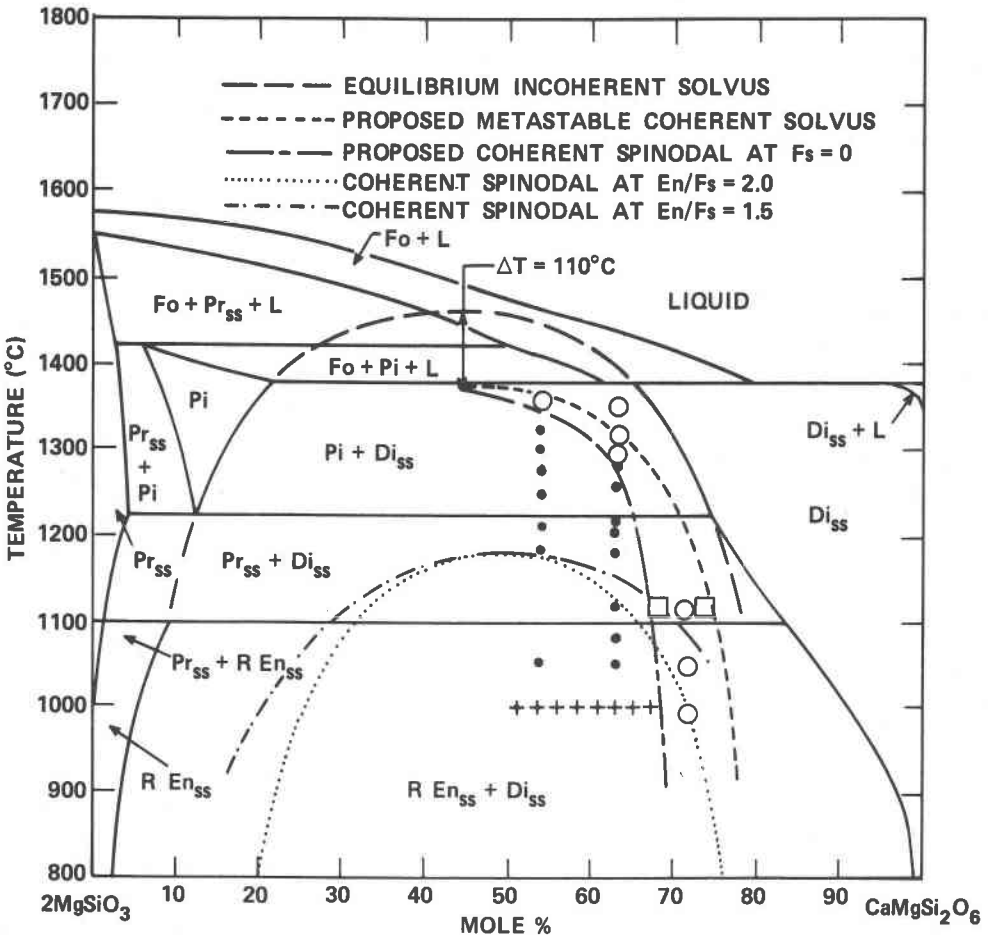

Fig. 1. Equilibrium diagram for Di($CaMgSi_2O_6$)–En($Mg_2Si_2O_6$) join replotted in mole percent (after Kushiro, 1972). The consolute point of the equilibrium solvus suggested by Yang (1973) is used as 1450°C along with the ΔT value of 110°C from Fletcher and McCallister (1974). The solid circles are the irregular lamellae observed in TEM by McCallister and Yund (1975, 1977) while the open circles and squares are their TEM data for compositions and annealing temperatures where lamellae were absent, rare, or of the type which were related to sample supersaturation. The superimposed symbol + indicates the range of compositions where modulated lamellae are observed in the clinopyroxenes of kimberlites (McCallister and Nord, 1981). The proposed coherent spinodal at Fs = 0 is from the data of McCallister and Yund (1977) and the coherent solvus is calculated from the coherent spinodal by the technique of Cook and Hilliard (1965). These compositions agree with the data of McCallister and Nord (1981) for the coherent solvus of subcalcic diopsides in kimberlites. The coherent spinodals of two iron-rich pseudobinary joins across the pryoxene quadrilateral at En/Fs = 2 (Lally et al., 1975) and En/Fs = 1.5 (Grove, 1982) are superimposed for comparison. A suggested metastable coherent solvus at Fs = O consistent with the above data is superimposed.

maximum spinodal wavelength is achieved quickly during annealing or continuous cooling. However, late stage spinodal decomposition[2] has been found to exhibit $t^{1/3}$ growth (Tsakalakos, 1977) as the decomposition fluctuations approach the stationary wavelength that minimizes the free energy[3] (Langer, 1971) within the coherent

[2] The combined use of analytic expressions and the analytic solution of Cahn's (1966) nonlinear diffusion equation at long wavelengths (later stage spinodal decomposition) are used to follow the behavior of a composition profile with time and to explain the subsequent growth ($t^{1/3}$) of the wavelength which is not predicted by the early stage linear spinodal theory (Cahn, 1961, 1962). The nonlinearity of the diffusion equation causes (1) the growth of higher harmonics for each wave ($1/\lambda$), and (2) a decrease in the rapid exponential growth of the fluctuation during early stage decomposition (Tsakalakos, 1977). The sharpening of the phase boundary near the spinodal is attributed to the influence of the higher harmonics of each wave ($1/\lambda$) "squaring off" the sinusoidal composition modulations (Tsakalakos, 1977). Tsakalakos' (1977) approach allows spinodal composition to be analyzed from the early to the later stage regimes as the wavelength approaches the stationary state (Langer, 1971).

[3] The "stationary state" of Langer (1971).

spinodal. The position of McCallister's (1978) composition ($Di_{54}En_{46}$) within the proposed Di–En coherent spinodal (1100–1300°C range of Fig. 1) solid circles is, therefore, consistent with a mechanism of later stage spinodal coarsening rather than an approach to the coherent solvus.

Recently, the use of coarsening slopes based on wavelength changes with time during isothermal annealing were compared with the experimental results of small-angle neutron scattering (Jantzen, 1978; Jantzen et al., 1981 a,b), via the kinetic Rundman-Hilliard (1967) analysis for spinodal decomposition and via the Porod (1951) analysis for delineation of nucleation and growth in order to distinguish between regimes of spinodal coarsening and nucleation and growth. At a given composition, annealing sequences yielded coarsening slopes approaching zero at temperatures corresponding to and above the spinodal boundary. As the temperature regime of the spinodal boundary is approached, the annealing sequences obey a $t^{1/3}$ rate law. Therefore, coarsening by nucleation and growth at $t^{1/3}$ (McCallister, 1978; Nord and McCallister, 1979; Nord, 1980) may be indistinguishable from spinodal coarsening at $t^{1/3}$ unless time-temperature annealing sequences are examined for each bulk composition.

The kinetic evolution of microstructures in natural pyroxenes is closely related to cooling rate (Grove, 1982; Nord and McCallister, 1979). However, the $t^{1/3}$ growth region of spinodal coarsening (coarsening of modulated structures) and the $t^{1/3}$ coarsening regime suggested by Nord and McCallister (1979) at the coherent solvus (coarsening kinetics in the region of nucleation and growth) may be difficult to distinguish. Both are diffusion-controlled processes. The distinction may, indeed, be (1) the size regime, e.g., in metallic systems lamellar coarsening is observed up to a wavelength of 1000Å (Butler and Thomas, 1970) while spinodal decomposition is of the 20-200Å regime; or (2) the time-temperature regime, e.g., comparisons of textures annealed 4 to 2200 hours for $Di_{54}En_{46}$ (McCallister, 1978) at 1300°C vs. 359 to 1600 hours for $Wo_{25}En_{31}Fs_{44}$ (Nord and McCallister, 1979 in Buseck et al., 1980) at 1000°C.

Incoherent vs. coherent equilibrium

The discussion of the compositional limitations of lamellar phases formed by spinodal decomposition vs. lamellar phases formed by nucleation and growth as given by Cameron and Papike (1981) demonstrates the existing confusion between coherent and incoherent equilibrium. The coherent phases formed by nucleation and growth can have the compositional limits of the coherent solvus before the incoherent equilibrium phases are formed: exsolution lamellae formed by coherent precipitation and growth may, therefore, not have the equilibrium composition. *Only* exsolution lamellae formed by incoherent nucleation and growth will have the equilibrium solvus composition on those coherent precipitates that have lost coherency. Spinodally formed lamellae or coherent lamellae formed by nucleation and growth would *not* reach the composition limits of the equilibrium incoherent solvus in a crystalline system unless (1) no strain existed, meaning that the lattice parameters of the exsolving phases were identical or (2) unless the exsolving phases lost their coherency after spinodal coarsening or coherent nucleation and growth, e.g., coarsening within the coherent solvus field.

A differentiation must be made between a coherent and an incoherent equilibrium phase diagram. The coherent phase diagram is always metastable and lies within the unstressed equilibrium phase diagram. The coherent phase diagram is a real, metastable phase diagram since it involves reversible metastable equilibrium, which is subject only to the constraint that the lattices remain continuous. The spinodal which leads to spontaneous decomposition is thus the spinodal of the coherent free energy curve of the metastable coherent phase diagram (Cahn, 1968). The interpretation of the coherent phase diagram is subtle and caution should be exercised when data are interpreted and subsequently quoted.

Conclusions

Theoretical treatments of spinodal decomposition are kinetic models of the decomposition mechanism. Use of morphologic or textural arguments to determine mechanistic changes during the solidification of alloy, ceramic, or mineralogic systems can be misleading. The literature on spinodal mechanisms in Fe-free proxene systems is confusing, but forms a consistent picture when the experimental data for iron-free and iron-enriched pyroxenes are compared and related to the more recent mathematical treatments of late-stage spinodal decomposition. In particular the following conclusions can be drawn:

(1) A coherent solvus in the iron-free pyroxene system can be calculated from the coherent spinodal of McCallister and Yund (1975) and other known experimental data.

(2) This coherent phase diagram is consistent with available experimental and textural data for synthetic and natural iron-free pyroxenes.

(3) Comparison with the data for iron-rich pyroxenes suggests that the width of the coherent spinodal constricts when the iron-free pyroxene join is approached.

(4) Late stage spinodal textures coarsen via a $t^{1/3}$ rate law and the Di_5En_{46} data (McCallister, 1978) between 1100–1300°C is consistent with the model of late stage spinodal coarsening rather than an approach to the coherent solvus.

(5) Coarsening by nucleation and growth at a $t^{1/3}$ rate and late stage spinodal coarsening at $t^{1/3}$ may be indistinguishable unless time-temperature sequences are examined; more experimental evidence is necessary to unequivocally attribute iron-free pyroxene textures to decomposition by a spinodal mechanism.

Acknowledgments

Special thanks are due G. L. Nord of the USGS and D. G. Howitt of the University of California at Davis for critically reviewing the manuscript.

References

Ardell, A. J., Nicholson, R. B. and Eshelby, J. D. (1966) Modulated structure of aged nickel-aluminum alloys. Acta Metallurgica, 14, 1295–1309.

Buseck, R. P., Nord, G. L., and Veblen, D. R. (1980) Subsolidus phenomena in pyroxenes. In C. T. Prewitt, Ed., Pyroxenes, Mineralogical Society of America Reviews in Mineralogy, Vol. 7, p. Mineralogic Society of America, Washington, D.C.

Butler, E. P. and Thomas, A. (1970) Structure and properties of spinodally decomposed Cu–Ni–Fe alloys. Acta Metallurgica, 18, 347–365.

Cahn, J. W. (1961) On spinodal decomposition. Acta Metallurgica, 9, 795–801.

Cahn, J. W. (1962) Coherent fluctuations and nucleation in isotropic solids. Acta Metallurgica, 10, 907–913.

Cahn, J. W. (1966) The later stages of spinodal decomposition and the beginnings of particle coarsening. Acta Metallurgica, 14, 1685–1692.

Cahn, J. W. (1968) Spinodal decomposition. Transactions American Institute Mining Engineers, 242, 166–180.

Cameron, M. and Papike, J. J. (1981) Structural and chemical variations in pyroxenes. American Mineralogist, 66, 1–50.

Champness, P. E. and Lorimer, G. W. (1973) Precipitation (exsolution) in an orthopyroxene. Journal of Materials Science, 8, 467–474.

Cook, H. E. and Hilliard, J. E. (1965) A simple method of estimating the chemical spinodal. Transactions of the American Institute Mining Engineers, 233, 142–146.

Fine, M. E. (1964) Phase Transformations in Condensed Systems. Macmillian Co., New York.

Fletcher, R. C. and McCallister, R. H. (1974) Spinodal decomposition as a possible mechanism in the exsolution of clinopyroxene. Carnegie Institute Washington Year Book, 73, 396–399.

Grove, T. L. (1982) Use of exsolution lamellae in lunar clinopyroxenes as cooling rate speedometers an experimental calibration. American Mineralogist, 67, 251–268.

Herman, H. and MacCrone, R. K. (1971) Comments on "Separation of phases by spinodal decomposition in the systems Al_2O_3–Cr_2O_3 and Al_2O_3–Cr_2O_3–Fe_2O_3." Journal of the American Ceramic Society, 55, 50.

Huston, E. L., Cahn, J. W. and Hillard, J. E. (1966) Spinodal decomposition during continuous cooling. Acta Metallurgica, 14, 1053–1062.

Jantzen, C. M. (1978) Spinodal decomposition and precipitation in rapidly quenched oxides: Ph.D. thesis. S.U.N.Y. at Stony Brook, Stony Brook, New York.

Jantzen, C. M. and Herman, H. (1978) Spinodal decomposition: Phase diagram representation and occurrence. In A. Alper, Ed., Phase Diagrams: Materials Science and Technology, p. 127–184. Academic Press, New York.

Jantzen, C. M., Schwahn, D., Schelten, J., and Herman, H. (1981a) The SiO_2–Al_2O_3 System. Part I. Later stage spinodal decomposition and metastable immiscibility. Physics and Chemistry of Glasses, 22, 122–137.

Jantzen, C. M., Schwahn, D., Schelten, J. and Herman, H. (1981b) The SiO_2–Al_2O_3 system. Part II. The glass structure and decomposition model. Physics and Chemistry of Glasses, 22, 138–144.

Kraft, W. (1973) Solidification structures of eutectic alloys. Metals Handbook, 8, 155–157.

Kushiro, I. (1972) Determination of liquidus relations in synthetic silicate systems with electron probe analysis: The system forsterite–diopside–silica at 1 atmosphere. American Mineralogist, 57, 1260–1271.

Lally, J. S., Heuer, A. H., Nord, G. L. Jr., and Christie, J. M. (1975) Subsolidus reactions in pyroxenes: an electron petrographic study. Contributions to Mineralogy and Petrology, 51, 263–282.

Langer, J. S. (1971) Theory of spinodal decomposition in alloys. Annals of Physics, 63, 53–86.

Laughlin, D. E. and Cahn, J. W. (1975) Spinodal decomposition in age hardening of copper–titanium alloys. Acta Metallurgica, 23, 329–339.

Mack, D. J. (1973) Nonferrous eutectoid structures. Metals Handbook, 8, 192–193.

Mangonon, P. L., Oakwood, T. G. and Shapiro, J. M. (1973) Ferrous eutectoid structures. Metals Handbook, 8, 188–191.

McCallister, R. H. (1974a) Kinetics of enstatite exsolution from supersaturated diopsides. In A. W. Hofman et al., Eds., Geochemical Transport and Kinetics, p. 195–204. Carnegie Institute Washington, Publication #634, Washington, D.C.

McCallister, R. H. (1974b) The exsolution kinetics of a diopside solid solution having the composition 54.1 mole% $CaMgSi_2O_6$, 45.9 mole% $Mg_2Si_2O_6$. Carnegie Institute Washington Yearbook, 73, 396–399.

McCallister, R. H. (1978) The coarsening kinetics associated with exsolution in an iron-free clinopyroxene: Contributions to Mineralogy and Petrology, 65, 327–331.

McCallister, R. H. and Nord, G. L. Jr., (1981) Subcalcic diopsides from kimberlites: Chemistry, exsolution microstructures, and their thermal history. Contributions to Mineralogy and Petrology, 78, 118–125.

McCallister, R. H. and Yund, R. A. (1975) Kinetics and microstructure of pyroxene exsolution. Carnegie Institute Washington Yearbook, 74, 433–436.

McCallister, R. H. and Yund, R. A. (1977) Coherent exsolution in Fe-free pyroxenes. American Mineralogist, 62, 721–726.

Newkirk, J. B. (1973) Structures resulting from aging and precipitation. Metals Handbook, 8, 175–183.

Nord, A. L. Jr. (1980) Decomposition kinetics in clinopyroxenes (abstr.) Geological Society of America Abstracts with Programs, 12, 492.

Nord, G. L. and McCallister, R. H. (1979) Kinetics and mechanism of decomposition in $Wo_{25}En_{31}Fs_{44}$ clinopyroxene. Geologic Society of America Abstracts with Programs, 11, 488.

Porod, G. (1951) Die Rontgen Kleinwinkelstreuung von dichtgepackten kolloiden systemen. Kolloid, 124, 83–114.

Rundman, K. B. and Hilliard, J. E. (1967). Early stages of spinodal decomposition in an aluminum-zinc alloy. Acta Metallurgica, 15, 1025–1033.

Seward, T. P., Uhlmann, D. R. and Turnbull, D. (1968). Development of a two phase structure in glasses with special reference to the system BaO–SiO_2. Journal American Ceramic Society, 51, 634–643.

Shewmon, P. G. (1969). Transformation in Metals. McGraw Hill Book Co., New York.

Tarshis, L. A., Walker, J. L. and Rutter, J. W. (1973). Solidifica-

tion structures of solid solutions. Metals Handbook, 8, 150–154.

Tsakalakos, T. (1977) Interdiffusion and enhanced elastic modulus effect in composition modulated copper–nickel-thin foils. Ph.D. Thesis. Northwestern University, Evanston, Illinois.

Yang, H. (1973). Crystallization of iron-free pigeonite in the system anorthite–diopside–enstatite–silica at atmospheric pressure. American Journal Science, 273, 488–497.

Yund, R. A. and McCallister, R. H. (1970) Kinetics and mechanisms of exsolution. Chemical Geology, 6, 5–30.

Manuscript received, July 14, 1981;
accepted for publication, October 13, 1983.